13

The effect of the substrate material on the structure, topology, composition, optical and mechanical properties of chemically deposited PbS films

© L.N. Maskaeva,[1,2] A.V. Pozdin,[1] V.F. Markov,[1,2] E.V. Mostovshchikova,[3] V.I. Voronin,[3] P.N. Mushnikov,[4] A.Yu. Pavlova[3]

[1] Ural Federal University after the first President of Russia B.N. Yeltsin,
620002 Yekaterinburg, Russia
[2] Ural Institute of State Fire Service of EMERCOM of Russia,
620062 Yekaterinburg, Russia
[3] M.N. Mikheev Institute of Metal Physics, Ural Branch, Russian Academy of Sciences,
620108 Yekaterinburg, Russia
[4] Institute of High-Temperature Electrochemistry, Ural Branch, Russian Academy of Sciences,
620066 Yekaterinburg, Russia
e-mail: andrej.pozdin@yandex.ru

Received February 17, 2024
Revised September 12, 2024
Accepted September 12, 2024

The article presents the results of comprehensive studies of the influence of the substrate material on the structure, composition, topology and optical properties of chemically deposited lead sulfide films using X-ray diffraction, electron and atomic force microscopy methods, with an estimation of the mechanical stresses arising in the volume of the films and at the film−substrate interface. It is found that the formation of the films on fused quartz and synthetic sapphire substrates occurs from crystallites with a predominant (111) crystallographic orientation, and on photo glass and microscope slide glass substrates — from crystallites with both (111) and (220) orientations. The effect of preliminary etching of substrates in HF acid on the surface topology and features of nucleation of the PbS films is discussed. It is concluded that the surface relief of lead sulfide films does not repeat the relief of the substrates. Using fractal formalism, it is shown that the formation of the PbS films on all studied substrates is described by a model of particle association of the cluster-particle type in three-dimensional space. A correlation is revealed between the number of nanoparticles in the PbS layer and the band gap of the material. An increase in the magnitude of compressive stresses at the film−substrate interface is found within the range from -53.9 to $-318.6\,\mathrm{kN/m^2}$ in the series slide glass−photo glass−sapphire−quartz.

Keywords: chemical bath deposition, thin films, lead sulfide, substrate material, morphology, crystal structure, mechanical stresses.

DOI: 10.61011/TP.2024.11.59758.39-24

Introduction

Lead sulfide thin films deposited using various physico-chemical technologies on substrates specially designed for this purpose have been commonly applied for the creation of highly sensitive photodetectors and photodetectors in the visible and near-infrared spectral ranges ($0.4-3.2\,\mu$m) [1–4]. They are also a promising material for the creation of high efficiency solar radiation converters [5], thermoelectric elements [6], optical switches [7], analyzers of components of gaseous media [8,9], biosensors and microbiological labels [10].

It is obvious that as there is a close relationship in the „film-substrate„ system, studying the structure, morphology, semiconductor and functional properties of deposited films in isolation from the substrate are of little promise. At the same time, both the composition and structure of the substrate material and the condition of its surface will have an impact. Important factors determining this relationship include the degree of surface roughness of the substrate, its reactivity (or inertia) to the film material and reagents used for preparation, mechanical strength, thermal conductivity and temperature resistance, differences in temperature coefficients of linear expansion of the film and substrate, dielectric and insulating properties, etc. Amorphous silicate, borosilicate, alkali-free and quartz glasses, synthetic sapphire, polycrystalline glass, ceramics are most widely used as substrate materials in modern technological applications, based on the purpose of films. It is important to note that researchers, as a rule, prefer the chemical deposition of PbS films from aqueous solutions (chemical bath deposition — CBD), which is a simple, economical and industrially scalable method for manufacturing high-quality semiconductor layers without the need for high temperatures and high vacuum [11–14].

The information about the effect of the substrate material (Si, Ge, GaAs, HfO_2, SiO_2, Al_2O_3) on morphology, crystal structure, electronic structure and optical properties of PbS films was analyzed in Ref. [15,16]. Mismatch of the crystal lattices of the substrate and the film, as well as the difference in their temperature coefficients of linear expansion, largely determines the adhesion strength of the film and the resulting mechanical stresses both in the volume and at the interface „film–substrate" [17]. The information obtained is sketchy, and characterizes only certain aspects of the influence of the substrate on the properties of the deposited layers. As for PbS films, optically transparent substrates based on glass [11,12,14,18,19], fused quartz [20–22] and synthetic sapphire [23] are the most commonly used for their chemical deposition. The choice of the substrate material is determined by both economic reasons (slide glass, photographic glass) and the search for the optimal option for solving a specific task based on understanding the impact of the substrate material on the functional properties of manufactured products. The use of quartz and sapphire as substrates is associated with their thermal and chemical stability, optical transparency in the ranges $(0.25-2.8)$ and $(0.17-5.5)\,\mu$m respectively [24,25], high insulating properties (resistivity $10^{11}-10^{15}\,\Omega\cdot$cm [26,27]), as well as a very low parasitic capacity, which ensures the performance of the developed devices [28]. A relatively high thermal conductivity ($\sim 23-25\,$W/(m·K) is additional advantage of synthetic sapphire [29]), which ensures heat dissipation from the optical elements of the device operating under high thermal loads.

Taking into account the undoubted contribution of the studies in Ref. [13,30] in the development of the method of CBD of semiconductor films, we would like to note that they still contain rather scarce information concerning the effect of substrates on the morphology and structural characteristics of chemically deposited PbS films, and very limited information about the arising mechanical stresses at the interface between the film and the substrate, although this issue is very relevant in connection with creation of functional devices for solar energy, sensors, opto- and nanoelectronics. There have been no comparative studies devoted to this problem to date, in particular, a comprehensive assessment of the effect of the substrate used on the composition, topology, crystal structure and functional properties of PbS films. The variety of influencing factors listed above does not allow a priori predicting the formation of certain morphological structures of films, as well as the nature of changes in their semiconductor properties.

In the light of the above, this paper is devoted to studying the impact of characteristics of the substrates used on the structural and morphological features, as well as on the optical properties of chemically deposited PbS films with an assessment of mechanical stresses in their volume and at the „film–substrate" interface.

1. Experimental part

PbS films were obtained by CBD from ammonium citrate aqueous solutions containing lead acetate $Pb(CH_3COO)_2$, sodium citrate $Na_3C_6H_5O_7$, ammonium hydroxide NH_4OH and thiourea $(NH_2)_2CS$ in the ratio of $0.07:0.5:7:1$ [8,12]. The films were deposited during 90 min at 353 K in TS-TB-10 thermostat in sealed molybdenum glass reactors. The accuracy of maintaining the synthesis temperature was $\pm 0.1^\circ$.

The lead sulfide films are formed by chemical deposition in an alkaline medium based on the following reaction:

$$PbL_x^{2+} + N_2H_4CS + 4OH^- = PbS\downarrow + xL + CN_2^{2-} + 4H_2O, \quad (1)$$

where L is the ligand for lead ions.

The substrates used in this study were fused quartz — an isotropic single-component compound consisting of SiO_2; a slide glass (72.2% SiO_2, 14.3% Na_2O; 1.2% K_2O, 6.4% CaO, 4.3% MgO, 1.2% Al_2O_3, 0.03% Fe_2O_3, 0.3% SO_3); photographic glass (72.5% SiO_2, 13.4% Na_2O; 0.5% K_2O, 8.0% CaO, 3.5% MgO, 1.5% Al_2O_3, 0.1% Fe_2O_3, 0.5% SO_3) and synthetic sapphire (99.9% of Al_2O_3,) with the crystal lattice type belonging to the hexagonal crystal system $3m$ with parameters $a = 4.758$ Å; $c = 12.991$ Å.

The substrate surface was treated before chemical deposition of the films for ensuring good adhesion to the substrates used, which included holding in a diluted solution of hydrofluoric acid HF (1 : 20) at room temperature for 5 s, then in a chromium mixture ($H_2SO_4 + K_2Cr_2O_4$) at 333 K for 20 min. The substrates were thoroughly rinsed with warm distilled water after each operation.

The thickness of the obtained films was evaluated by interference microscopy using Linnik MII-4M microinterferometer. The thickness of lead sulfide PbS films deposited on the studied substrates so determined was $(450-485) \pm 20$ nm.

Phase and structural analysis of synthesized thin films PbS was performed by X-ray diffraction (XRD) using Rigaku MiniFlex600 diffractometer (Rigaku, Japan) with a copper anode CuK_α in the range of angles $2\theta = 20-120^\circ$ with a step of 0.01° and scanning time 10 s at a point. The full-profile Rietveld analysis [31], implemented in the FullProf Suite program [32] was used for the description of experimental X-ray patterns. The scale factor, the spectrum zero shift, the deviation from the scattering plane and Debye–Waller thermal factor were preliminarily determined during calculations, and the Chebyshev polynomial was used to describe the X-ray patterns background [33].

The magnitude of the average internal microstresses (S) resulting from deformation of the crystal lattice of PbS films was estimated using the formula [34]:

$$S = [(a_0 - a)/a_0] \cdot E_{PbS}/2\nu_{PbS}, \quad (2)$$

where a_0 — the crystal lattice parameter of coarse-grained PbS, equal to 0.5936 nm; a — the crystal lat-

tice parameter of the PbS film obtained in the paper; Young's modulus $E_{\mathrm{PbS}} = 70.2\,\mathrm{GPa}$ [35], Poisson's ratio $\nu_{\mathrm{PbS}} = 0.28$ [35].

The surface morphology and elemental composition of the films were studied by scanning electron microscopy (SEM) using Tescan Vega 4 LMS microscope with energy dispersive X-ray spectroscopy (EDS) Oxford Xplore EDS−AZtecOne. The particle size was determined using the Measurer software.

The topology and surface relief of substrates and films was studied using atomic force microscopy (AFM) in semicontact mode using a scanning probe microscope Ntegra Aura (NT-MDT, Russia), probes NSG01 (NT-MDT, Russia) with a radius of curvature of no more than 20 nm. At the same time, the magnitude of the oscillation amplitude of the cantilever was 40−60% of the amplitude of free oscillations and satisfied the condition of coincidence of the phase curves of input−output curves at this operating point. The surface was scanned with a resolution of at least 512×512 points with sweep line frequency of 1 Hz.

The fractal dimension of the studied PbS films was determined by computer processing of AFM images in the program Gwyddion-2.55 using the methods of cube counting D_c and triangulation D_t [36].

Optical studies of thin-film layers were carried out in the near-IR range 0.3−0.95 eV using an automated cryomagnetic system based on a prism IR spectrometer. The system includes a source of incoherent LC4-12 IR radiation with a temperature of 1100°C, a monochromator with dispersing elements in the form of prisms made of NaCl and glass (F1) and a radiation receiver — a bismuth bolometer with sensitivity of 10^{-11} W. The resolution of the system is 0.01 eV, the minimum recorded light transmission signal is 10^{-4}. The absorption spectra $\alpha(E)$ were calculated from the experimentally obtained transmission spectra $t(E)$ without taking into account reflection according to the formula

$$\alpha(E) = \frac{1}{h_{\mathrm{PbS}}} \ln\left(\frac{1}{t(E)}\right), \tag{3}$$

where h_{PbS} — film thickness, $t(E) = I/I_0$ — film transmission, I, I_0 — intensity of light transmitted through the film and through the substrate, respectively.

Since single-crystal lead sulfide PbS [37] is a semiconductor with a direct energy band, the dependence of the absorption coefficient on the energy in the region of the edge of fundamental absorption is expressed by the formula

$$\alpha = \frac{[A(\hbar\omega - E_g)]^{1/2}}{\hbar\omega}, \tag{4}$$

where $\hbar\omega$ — photon energy, $A = \mathrm{const}$ — frequency independent coefficient, E_g — the value of the band gap. It can be seen from the formula (4) that this dependence can be transformed to the form

$$(\alpha \cdot \hbar\omega)^2 = A \cdot (\hbar\omega - E_g), \tag{5}$$

which allows determining the value of E_g from the extrapolation of the linear portion of the absorption spectrum plotted in coordinates $(\alpha E)^2 - E$ on the abscissa axis.

An approximate assessment of mechanical stresses $\sigma_{\Delta\alpha}$ in a two-layer structure „PbS film−substrate" under the condition $h_{substr} \gg h_{\mathrm{PbS}}$ was carried out according to the formula proposed in Ref. [38]:

$$\sigma_{\Delta\alpha} = \frac{6 \cdot E_{\mathrm{PbS}} \cdot (\beta_{substr} - \beta_{\mathrm{PbS}}) \cdot h_{\mathrm{PbS}} \cdot \Delta T}{(1 - \nu_{\mathrm{PbS}}) \cdot (3h_{substr} - 4h_{\mathrm{PbS}})}, \tag{6}$$

where E_{PbS} — Young's modulus for lead sulfide PbS ($E_{\mathrm{PbS}} = 70.2\,\mathrm{GPa}$) [35]; β_{substr}, β_{PbS} — temperature coefficients linear expansion of the substrate and film ($\beta_{\mathrm{PbS}} = 19 \cdot 10^6\,\mathrm{K}^{-1}$) [35]; ΔT — temperature difference; ν_{PbS} —Poisson's ratio films ($\nu_{\mathrm{PbS}} = 0.28$) [35]; h_{substr}, h_{PbS} — substrate and film thicknesses, respectively.

2. Results and discussion

2.1. X-ray diffraction analysis of films

X-ray patterns of PbS films deposited on quartz, photographic glass, slide glass and sapphire (Fig. 1) show diffraction reflections of only one phase having a face-centered cubic lattice of the NaCl type ($B1$, sp. gr.). The observed different ratio of the experimental intensities of diffraction reflections in X-ray patterns is due to the different predominant crystallographic orientation of the crystallites in the studied films, therefore, their texturization was taken into account to describe the X-ray images. The best agreement of the calculated and experimental data for films deposited on substrates of fused quartz and sapphire was obtained under the condition of the preferred orientation of the grains in the direction (111), and for films deposited on photographic glass and slide glass, two orientations — in the directions (111) and (220). Taking into account the texture allowed obtaining a minimum difference between the profiles of the experimental and calculated X-ray patterns of the studied PbS films on different substrates (Fig. 1), which confirms the correctness of the chosen model and the high accuracy of the performed full-profile analysis.

The determined structural characteristics of PbS films, calculated taking into account two models of the predominant orientation of crystallites in them, are given in Table 1.

As can be seen from Table 1, the formation of films deposited on substrates of fused quartz and sapphire occurs entirely from crystallites with a predominant orientation in the direction of (111) relative to the substrate, and on photographic glass and slide glass, in addition to crystallites with an orientation of (111), the content of which is 64.5 and 79.1%, crystallites with an orientation of (220) are present. The lattice parameters of lead sulfide films on the substrates used in the work for crystallites with an orientation of (111) are close and range from 0.593375(3) to 0.593559(2) nm. Films deposited on photographic glass and slide glass are formed from crystallites of two orientations, and the

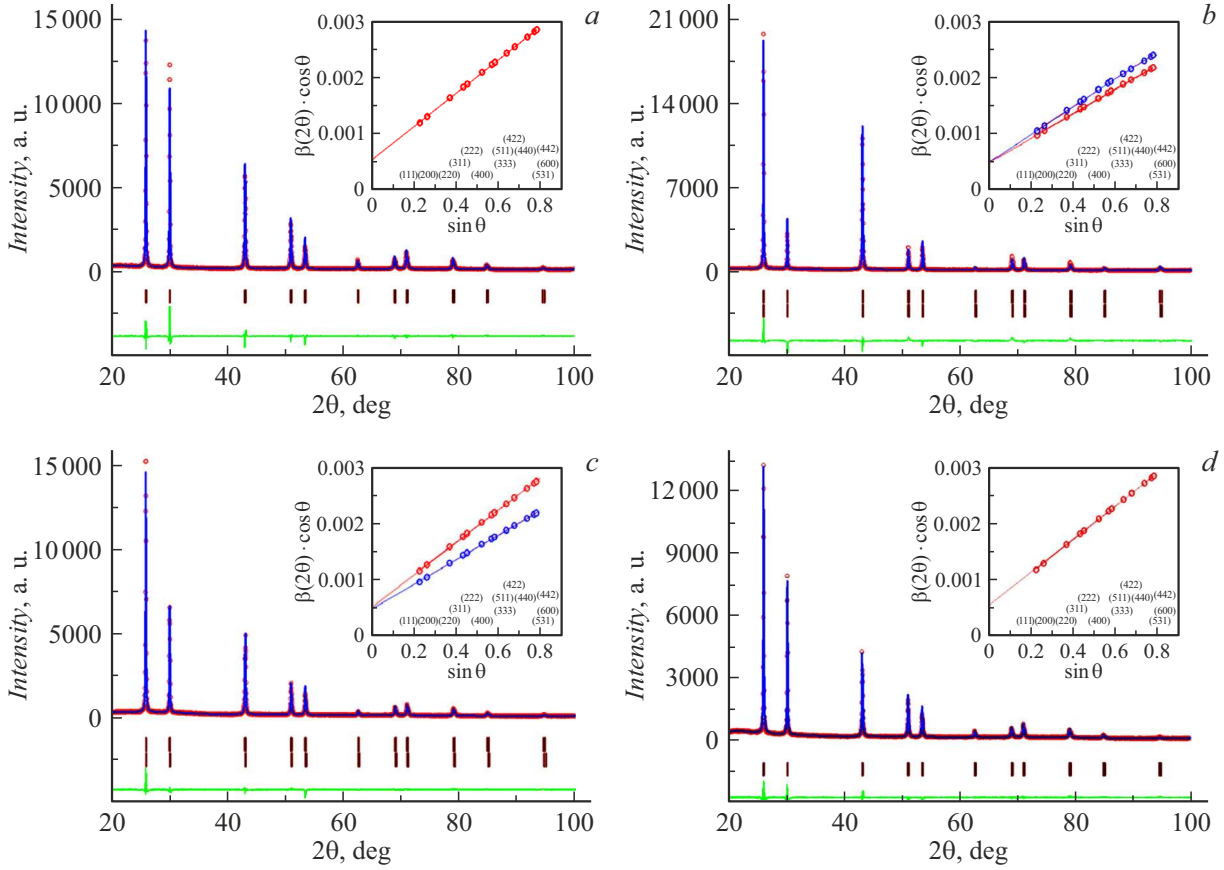

Figure 1. Experimental (circles) and calculated (envelope line) X-ray patterns of PbS films deposited on substrates of fused quartz (a), photographic glass (b), slide glass (c), sapphire (d). The difference between the experimental and calculated X-ray patterns is shown in the lower part of the figure. The strokes show the angular positions of the reflexes of the cubic phase $B1$. The inserts show the dependence of $\beta(2\theta) \cdot \cos\theta$ on $\sin\theta$ for grains with preferential orientation $(111)_{B1}$ (red) and $(220)_{B1}$ (blue).

Table 1. The crystal lattice parameter (a), the proportion of grains with preferential orientation (111) and (220), respectively, ($T_{(111)}$) and ($T_{(220)}$), the average value of microdeformations ($< \Delta d/d >$), the size of the coherent scattering regions CSR (D), the phase content with orientation (111) and (220) (%), internal microstresses (S) occurring due to deformation of the crystal film grids PbS

Type of substrate	Fused quartz	Photographic glass	Slide glass	Synthetic sapphire
		(111)		
a, nm	0.593494(5)	0.593463(4)	0.593559(2)	0.593375(3)
$T_{(111)}$, %	12.0	71.9	42.2	24.4
% of phase	100	64.5	79.1	100
$\Delta d/d \cdot 10^4$	10.9	7.5	10.3	10.9
D, nm	260	290	263	260
$S \cdot 10^4$, kN/m^2	2.23	2.88	0.86	4.73
		(220)		
a, Å	–	5.93390(2)	5.93022(7)	–
$T_{(220)}$, %	–	49.5	52.3	–
% of phase	–	35.5	20.9	–
$\Delta d/d \cdot 10^4$		8.6	7.6	
D, nm		278	290	–
$S \cdot 10^{-4}$, kN/m^2		4.42	12.2	

parameter for crystallites with orientation (220) is less than for crystallites with orientation (111), and is 5.93390(2) and 5.93022(7) nm, respectively.

It is known that one of the main reasons for the broadening of X-ray pattern reflections is the small grain size (more precisely, the coherent scattering region CSR) D and micro-deformations in the volume of the material $\Delta d/d$. Insets in Figure 1 shows the dependence $\beta(2\theta) \cdot \cos\theta$ on $\sin\theta$ for grains with a predominant orientation (111) (red) and (220) (blue), which made it possible to separate the dimensional and deformation contributions to the broadening of reflections, performed using Williamson–Hall extrapolation method [39]. As a result, it was found that the films deposited on fused quartz and sapphire were formed from crystallites with the same CSR size $D = 260$ nm and microdeformation values $\Delta d/d$ $(10.9 \cdot 10^{-4})$; crystallites with orientation (111) have similar values $D = 263$ nm and $\Delta d/d = 10.3 \cdot 10^{-4}$ in the film on the slide glass, and crystallites with orientation (220) have slightly larger CSR size ($D = 290$ nm) and have a smaller value of microdeformations ($\Delta d/d = 7.6 \cdot 10^{-4}$). The PbS film deposited on photographic glass is somewhat different: crystallites with orientation (111) have a larger CSR size (290 nm) and a lower value $\Delta d/d$ $(7.5 \cdot 10^{-4})$ than crystallites (220), namely D (278 nm) and $\Delta d/d = (8.6 \cdot 10^{-4})$.

Deviations of the crystal lattice parameters a of films deposited on the substrates under discussion (Table 1) from the lattice parameter of the bulk PbS sample ($a_0 = 0.5936$ nm) should be noted. This difference indicates the occurrence of deformation during CBD due to internal microstresses S, the magnitude of which was estimated by formula (2). Maximum $(12.2 \cdot 10^4\ \mathrm{kN/m^2})$ and minimum $(0.86 \cdot 10^4\ \mathrm{kN/m^2})$ internal microstresses S were obtained in crystallites with orientation in the direction (220) and (111) in a lead sulfide film deposited on a slide glass. This is attributable to a decrease to 5.93022(7) and 0.593559(2) nm of the crystal lattice constant of a part of the crystallites with orientation in the direction of (220) and (111). A smaller difference in the lattice parameter was found on the remaining substrates, therefore, the internal micro-stresses are in the range from 2.23 to $4.73 \cdot 10^4\ \mathrm{kN/m^2}$.

These results indicate that internal microstresses in the films obtained in this work on a glass substrate are 3–6 times lower than internal microstresses determined by the authors of the publication [40] for PbS films chemically deposited on the same substrates, as well as approximately 9 times lower than internal microstresses in lead sulfide nanocrystals [41].

2.2. Morphological features and composition of PbS films

Despite the formation of PbS films in the same chemical deposition conditions (substrate surface treatment, composition of the reaction mixture, temperature and duration of the process), morphological features and the elemental composition of the films PbS were studied for obtaining a complete picture of their formation on the studied substrates, in addition to the structural state (crystal lattice parameter, preferential orientation, internal microstresses) of the formed phase.

It is known that the lead sulfide film is deposited under nonequilibrium conditions because of the high rate of conversion of metal salts into sulfide at the initial stage of the process ($\sim 11.7-12.1$ nm/min). As a result, the films are polycrystalline at the end of synthesis (90 min) and consist of tightly adjacent well-faceted crystallites in the form of three- and four-angle prisms with different size and crystallographic orientation relative to the surface plane of the substrate. Confirmation is provided by electron microscopic images of layers deposited on substrates of fused quartz, photographic glass, slide glass and sapphire (Fig. 2). The growth of crystallites with an energetically advantageous preferential orientation of (111) (red circles) is realized in PbS films on fused quartz and sapphire (Fig. 2, *a, d*) against the background of the chaotic orientation of the grains. However, PbS films deposited on photographic glass and slide glass substrates consist of crystallites of two types of crystallographic orientation (111) (red circles) and $(220)_{B1}$ (green lines) , as can be seen from Fig. 2, *b, c*.

Histograms of the distribution of crystallites forming the PbS film indicate its different granulometric composition on the substrates under discussion. A clear bimodal distribution of crystallites in size is observed only in a PbS film deposited on fused quartz (99.9% SiO_2): there are two maxima on the histogram: for crystallite sizes 350–550 nm ($\sim 30\%$) and 850–1000 nm (40%). In turn, crystallites of larger sizes ($1.1-1.4\,\mu$m) account for 9% (Fig. 2, *a*). The high proportion of large-sized crystallites is probably attributable to the presence of a significant energy barrier during the formation of a film on an amorphous substrate in the absence of a large number of active centers. Therefore, the process of nucleation on the surface of fused quartz takes place with the participation of a relatively small number of nuclei, the role of which is presumably performed by particles of products of hydrolysis of silicon tetrafluoride SiF_4 formed as a result of preliminary etching of the substrate surface in hydrofluoric acid [42]:

$$SiO_2 + 4HF = SiF_4 + 2H_2O \quad \Delta_r G^o_{298} = -90.5\ \mathrm{kJ/mol}. \tag{7}$$

The size distribution of crystallites in films obtained on photographic glass (74% SiO_2) and slide glass (72.2% SiO_2) can be considered as monomodal. The maximum particle distribution on the surface of the photographic glass corresponds to the dimensions of 300–500 nm ($\sim 59\%$) with 1% of nanoparticles (Fig. 2, *b*). The shape of the crystallites in the PbS film deposited on the slide glass does not change, but their sizes decrease to 250–400 nm ($\sim 53\%$) with a content of up to 3% nanoparticles (Fig. 2, *c*). The formation of smaller crystallites on amorphous substrates made of slide glass and photographic glass compared with a substrate made of fused quartz is due to a more developed microrelief

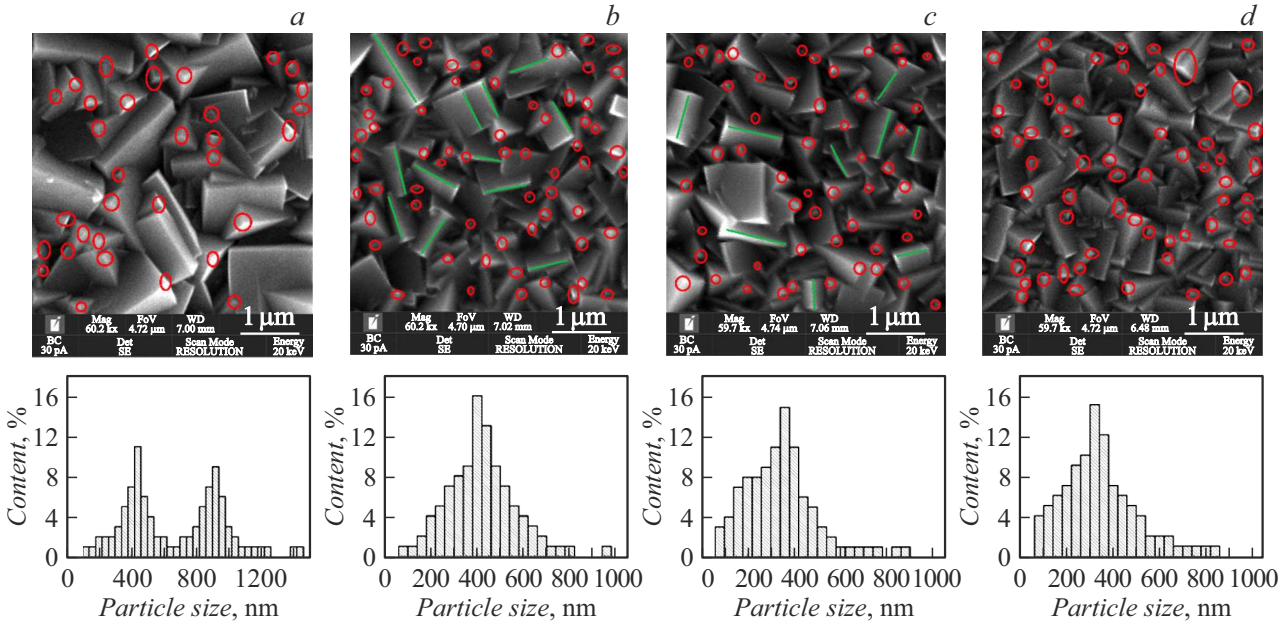

Figure 2. Electron microscopic images of PbS films chemically deposited on substrates of fused quartz (*a*), photographic glass (*b*), slide glass (*c*), sapphire (*d*) and dimensional distributions of crystallites in them. Crystallites with crystallographic orientation (111) are marked with red circles, and crystallites with crystallographic orientation (220) are marked with green lines in micrographs.

of their surface due to the selective interaction of an etchant (hydrofluoric acid), in addition to silicon dioxide, with Na_2O (14.3 and 13.4%) and CaO (6.4 and 8.0%) contained in the substrates [43]:

$$Na_2O + 2HF \rightarrow 2NaF + H_2O, \quad (8)$$

$$CaO + 2HF \rightarrow CaF_2 + H_2O. \quad (9)$$

Taking into account the percentage of oxides SiO_2, Na_2O and CaO in the composition of the substrates, the calculated values of the Gibbs energy change for standard conditions $\Delta_r G^o_{298}$ based on the thermodynamic characteristics of substances involved in reactions (7)–(9) [44], showed that substrates can be arranged in the following row with the increase of the free energy in the processes of interaction with hydrofluoric acid: fused quartz (-90.5 kJ/mol) $\rightarrow$ photographic glass (-139.64 kJ/mol) $\approx$ slid0e (-140.43 kJ/mol). The results of calculation of $\Delta_r G^o_{298}$ suggest the possibility of spontaneous occurrence of the above etching reactions, which in fact implies a corresponding change of the microrelief of the surface and an increase of the number of nucleation centers.

A lead sulfide film is formed on a sapphire, which is a crystalline material of hexagonal crystal system 3*m* from crystallites of a smaller size compared to the film obtained on quartz as can be seen from the results of electron microscopy. The probable reason for this is the presence of a larger number of nucleation centers on its surface, which is attributable to the crystal structure of sapphire and the its intensive etching in hydrofluoric acid, which contributes to a change of the microrelief of the surface:

$$Al_2O_3 + 6HF \rightarrow 2AlF_3 + 3H_2O. \quad (10)$$

A sufficiently high calculated value of the Gibbs energy change $\Delta_r G^o_{298}$ (-340.7 kJ/mol) is an indirect confirmation of this interaction. It should be noted that, unlike quartz and glass substrates, the final product of the reaction is a highly soluble compound AlF_3, as well as the possible formation of durable aluminum fluoride complexes. Based on this and due to the crystal structure of the sapphire surface, the PbS film consists of $\sim$ 52% crystallites with a size of 150–400 nm and contains $\sim$ 4%nanoparticles (Fig. 2, *d*).

The analysis of the obtained results allows making a conclusion that the revealed morphological features of the deposited lead sulfide films are determined by various conditions of nucleation and growth of the solid phase on the substrates used.

The content of the main elements in the PbS film deposited on the studied substrates was determined using elemental energy dispersion microanalysis over the entire surface area at least in 10 points. The results obtained indicate a slight nonstoichiometry of the synthesized films as can be seen from Table 2. Moreover, a slight decrease of the lead content (from 50.8 to 50.2 at.%) and an increase of the amount of sulfur (from 45.8 to 47.4 at.%) with a simultaneous decrease of the oxygen concentration from 3.4 to 2.2 at.% in films is observed in the series fused quartz $\rightarrow$ photographic glass $\rightarrow$ slide glass $\rightarrow$ synthetic sapphire.

It should be noted that the presence of oxygen in PbS films is virtually inevitable in case of chemical deposition on

Table 2. Elemental composition of PbS films synthesized on various substrates

Substrate material	Element content, at.%		
	Pb±0.5	S±0.4	O±0.2
Fused quartz	50.8	45.8	3.4
Photographic glass	50.5	46.5	3.0
Slide	50.7	47.2	2.1
Synthetic sapphire	50.2	47.3	2.5

substrates of an oxide nature. This is attributable both to the composition and subsequent transformation of the various oxygen-containing phases ($Pb(OH)_2$, PbO, $PbCO_3$, $PbSO_4$) formed during deposition [45–47], and to the formation of ion radical forms O^{2-} and OH^- at the interphase boundaries [48].

The deposition of the lead hydroxide phase is confirmed by the results of a thermodynamic assessment of the boundary conditions of its formation for the synthesis conditions used [13]. According to many researchers [13,30,49], the active nucleation of PbS films with high adhesion to the substrate occurs on its surface only in cases when a colloidal form of metal hydroxide is formed in the reaction mixture. Adsorbed colloidal hydroxide particles ensure the formation of nucleation centers and subsequent film growth as a result of sulfidization. An important (sometimes decisive) contribution to this process can be made, as will be shown below, by the resulting products of etching of substrates during their preparation for synthesis, which should presumably include slightly soluble hydrolysis products of silicon tetrafluoride and calcium fluoride.

2.3. Topology and fractal dimension

It is known that the surface roughness of the substrate is one of the main factors affecting both the mechanical and functional properties of deposited semiconductor films. We did not determine the roughness of the initial surface of the studied substrates. The surface roughness of the substrates used in the study is different according to literature sources, in particular, it ranges from 1.3 to 3−5 nm [24,50] and even up to 6 nm for fused quartz [51]. This characteristic is within the range of 15.6−19.3 nm for slide glass [52,53], and within the range of ∼ 20 nm for photographic glass [54]. The surface of the sapphire has a minimum roughness of less than 0.5 nm [55].

The etching was performed in a dilute solution of hydrofluoric acid HF (1 : 20) at room temperature for 5 s to increase the surface roughness of the substrates used for ensuring good adhesion of the PbS film to them.

A series of AFM images of the microrelief of the substrate surface after etching (upper row) and after deposition of PbS films on them (lower row) are shown in Fig. 3. A qualitative analysis of the results of AFM studies makes it possible to see that, firstly, the scanning areas with the size of 4×4 and $10 \times 10\,\mu$m demonstrate the scale dependence of the microrelief of both the substrate surface and films; secondly, the relief the film coating does not replicate the relief elements of the substrate.

Three of the studied substrates are X-ray amorphous, consisting either entirely of silicon dioxide SiO_2 (fused quartz), or containing it in the amount of 74.0% (photographic glass) and 72.2% (slide glass). Hence, it can be assumed that the mechanism of formation of lead sulfide films on them will be similar, but have their own characteristics depending on the substrate material. As already noted, the etching of these substrates in HF can result in the formation of products of hydrolysis of silicon tetrafluoride SiF_4 in the form of lead and ammonium hexafluorosilicates [56], evenly distributed over the surface of fused quartz and acting as centers of nucleation and growth of PbS films. We would like to remind that photographic glass and slide glass also contain sodium oxides Na_2O, potassium K_2O and calcium CaO in addition to SiO_2. Interaction of CaO with hydrofluoric acid by reaction (7) can facilitate the formation of insoluble calcium fluoride CaF_2 with a fluorite crystal structure ($a = 0.5463$ nm). It should be noted that the resulting sodium and potassium fluorides are soluble in the reaction mixture, which will lead to etching of these compounds from the substrates, providing them a more developed surface microrelief compared to fused quartz. Thus, the difference of the composition of the substrate material determines their microrelief of the surface after etching.

After etching, clearly ordered tetrahedral columnar formations up to ∼ 62−64 nm appeared on the surface of the quartz substrate (Fig. 3, *a, e*), and the surfaces of both glass substrates were covered with numerous needle-like structures tightly adjacent to each other up to 69−71 nm on photographic glass (Fig. 3, *b, f*) and 75−84 nm on slide glass (Fig. 3, *c, g*). It can be assumed that in the first case, the columnar formations are based on products of hydrolysis of SiF_4, and in the second case the columnar formations are based on a combination of products of hydrolysis of SiF_4 with calcium fluoride CaF_2 of a crystalline structure providing a high density of needle-like structures. The resulting inhomogeneities will act as centers of nucleation and growth of the PbS phase on the substrates under discussion, and their geometry will provide the morphology and crystal structure of the deposited films with specific features. It can be seen that photographic glass and slide glass substrates are characterized by a higher density of needle-like protrusions than a fused quartz substrate, which was probably the main reason for the formation of lead sulfide films from smaller crystallites with orientations (111) and (220), observed both in Fig. 2, *b, c*, and in Fig. 3, *b, c, f, g*.

Sapphire which is chemically relatively inert to HF retains a fairly smooth surface after etching. However, the roughness of the PbS film deposited on the sapphire substrate is close to the roughness of the film on the slide glass (Fig. 3, *c, g* and 3, *d, h*).

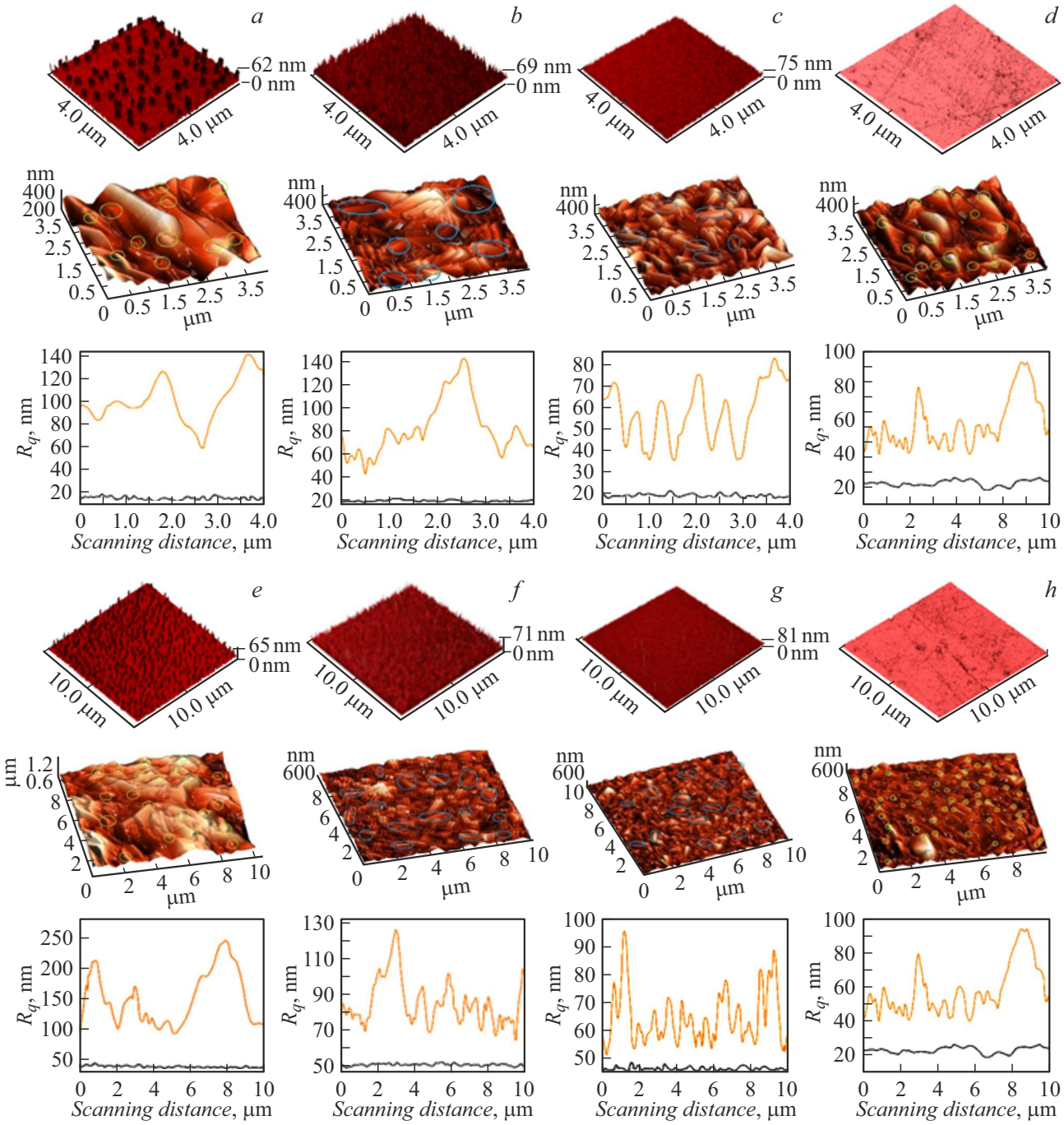

Figure 3. AFM images of substrates after etching in hydrofluoric acid, after deposition of PbS films on them and profiles of the RMS roughness of the substrates (black curve) and films (brown curve). Substrate material: fused quartz (*a, e*), photographic glass (*b, f*), slide glass (*c, g*), sapphire (*d, h*). Scan areas $4 \times 4\,\mu$m (*a*–*d*) and $10 \times 10\,\mu$m (*e*–*h*).

A quantitative analysis of AFM images was carried out simultaneously with a qualitative discussion of the surface relief of substrates and PbS films deposited on them. To this end, metric roughness parameters were calculated, including the RMS roughness R_q, characterizing the height of the surface profile, the maximum height of the profile R_z, i.e. the height difference between the uppermost and lowest points of the surface profile, and the asymmetry coefficient R_{sk}, determining the symmetry of the distribution of the surface profile relative to the midline.

For clarity, Figure 3 shows the profiles of the RMS roughness R_q of AFM images of the surface of substrates (black curves) and PbS films (brown curves) deposited on these substrates. The roughness increases by 3.5 and 3.7 times after application of the film to photographic glass and slide glass substrates, and

it increased by about 5–6 times on quartz and sapphire. The maximum profile height R_Z of the surface of PbS films decreases linearly from 512 to 440 nm ($4 \times 4\,\mu$m) and from 580 to 480 nm ($10 \times 10\,\mu$m) in a row of fused quartz → photographic glass → slide glass → sapphire.

The structure asymmetry coefficient R_{sk} differs from zero, so it can be said that the distribution of crystallites is uneven relative to the center of the studied area, and its positive values 0.48–0.66 and 0.41–0.61 indicate the presence of bulges on the relief of areas with sizes 4×4 and $10 \times 10\,\mu$m of the surface of PbS films deposited on all the studied substrates.

The value of the fractal dimension of the surface allows quantifying the degree of surface development using the position of the fractal theory [57], as well as drawing a conclusion about a possible mechanism for the formation of structures. If the fractal dimension values for the scan areas of 4×4 and $10 \times 10\,\mu$m obtained using the cube counting method are practically the same (2.31 ± 0.03 and 2.33 ± 0.03), then the range of values D_t found by the triangulation method is somewhat broader: 2.36 ± 0.03 and 2.43 ± 0.02. According to the accepted classification [58], the value of the fractal dimension with $D > 2.3$ assumes the growth of films on the substrate in case of Brownian motion and the probability of adhesion close to unity by the aggregation mechanism „cluster–particle“ (Diffusion Limited Aggregation — DLA). In this case, the primary clusters formed in the volume of the reaction mixture are deposited on the inhomogeneous surface of the substrate, sequentially covering it entirely, and they become larger by the addition of new particles from the solution [59]. For instance, based on the morphological features of the substrates, defects in the microstructure and surface exposures of the pores can be potential ways of local formation of a system of fixed nucleation centers and their island growth [60].

Despite the fact that the topology of lead sulfide films does not replicate the topology of the substrates, the surface of the PbS film grown on sapphire still remains more smooth and level having minimal roughness compared to other substrates. A film obtained on a substrate of fused quartz has the maximum value of the RMS roughness and the maximum profile height; the intermediate position is occupied by films deposited on substrates of photographic glass and slide glass. Thus, the substrate material and their geometric characteristics at the microlevel determine both the surface roughness of the lead sulfide films deposited on them and their morphology.

2.4. Optical properties

The band gap width is one of the parameters determining the properties of semiconductor materials, including lead sulfide. At the same time, this parameter can be affected not only by modification of the chemical composition by doping, but also by changes of the size of the crystallites that form the studied material. In particular, it is known that PbS is characterized by a significant increase of the band gap width („blue shift“ of the absorption edge) with a decrease of the grain size [61]. It was noted above based on a comparison of the CSR sizes and the roughness of the obtained films that the substrate material affects the size of the crystallites from which the film is formed. The transmission spectra of the films were measured to determine the evolution of the band gap in PbS films, depending on the type of substrate.

The absorption spectra $\alpha(E)$ of the studied PbS films on different substrates are shown in Fig. 4. The increase of the absorption coefficient observed in the spectra with an increase of the energy is associated with the onset of fundamental absorption (the band gap width of (single-crystal) lead sulfide PbS is ~ 0.4 eV [37]). It should be noted that a weak absorption band is visible in the spectra of $\alpha(E)$ films deposited on photographic glass and slide glass with a maximum at $E \approx 0.35$ eV, the intensity of which depends on the type of substrate. This band is shifted to the region of high energies in the absorption spectrum of a film on a sapphire substrate, and it has the highest intensity and merges with the beginning of the absorption edge in a film on a quartz substrate. The films studied in this paper are characterized by a sulfur deficiency (there are sulfur vacancies) and the existence of an admixture of oxygen as shown by elemental analysis (Table 2). Both of these types of defects can produce impurity bands near the absorption edge of lead sulfide [62], which are located in the region 0.3–0.4 eV depending on the type of defect, and their different ratios change the intensity of the impurity bands.

The absorption coefficient spectra were plotted in the coordinates $(\alpha E)^2 - E$ to estimate the band gap width, and the values of the band gap E_g were estimated from the extrapolation of the linear part of the obtained curve to the abscissa axis (Fig. 4, *b*). The values E_g obtained so amount to 0.40 ± 0.01 eV (fused quartz), 0.45 ± 0.01 eV (photographic glass) and 0.48 ± 0.01 eV (slide glass, sapphire). It should be noted that the value of the band gap width of the film on a quartz substrate is close to the value of the single crystal PbS. This is probably attributable to the formation of large crystallites in this film with a size of $\sim 1\,\mu$m (Fig. 2, *a*). A slight increase of the band gap width in films on other substrates is attributable to the fact that they are formed from submicron grains, and also a small content of nanocrystallites is observed in these films and it increases in films on a slide glass and on sapphire to 3–4%.

It should be noted that the type of absorption spectra as a whole and the band gap width vary insignificantly despite the formation of textures of crystallites of different character for films on the studied substrates, as well as their differing roughness, which was established using AFM, and different values of internal stresses in films estimated earlier. This suggests that these stresses are insignificant for a significant transformation of the zone structure.

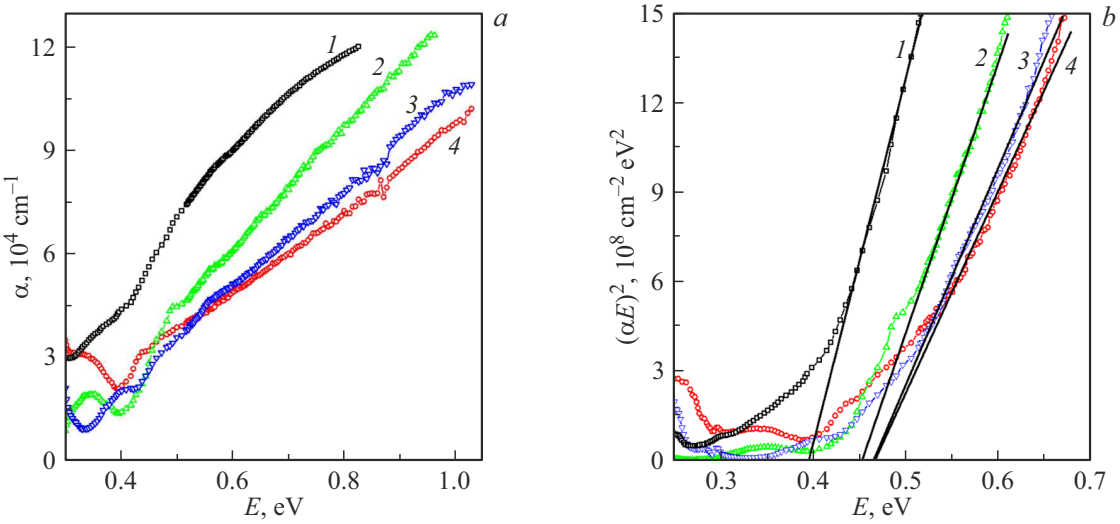

Figure 4. *a* —absorption spectra of PbS films deposited on a substrate of fused quartz (*1*), photographic glass (*2*), slide glass (*3*) or sapphire (*4*); *b* —absorption spectra plotted in coordinates $(\alpha E)^2 - E$.

Table 3. Temperature coefficient of linear expansion β of substrates [35], thickness of substrate (h_{substr}) and film (h_{PbS}), mechanical stresses at the interface „PbS film−substrate“ $\sigma_{\Delta\alpha}$

Material of substrate	$\beta \cdot 10^{-6}, \mathrm{K}^{-1}$	$h_{substr}\ 10^6$, nm	h_{PbS}, nm	$\sigma_{\Delta\alpha}$, kN/m^2
Fused quartz	0.56	0.31	485	−318.6
Sapphire	6.66	0.3	480	−212.4
Photographic glass	8.1	0.29	450	−181.4
Slide	8.3	1.0	470	−53.9

2.5. Mechanical stresses at „film−substrate“ interface

The mechanical stresses arising in thin films are conditionally divided into two groups according to L.B.Freund et al. [63]. The first category includes the so-called internal stresses (growth stresses), calculated by us in the study of the crystal structure of PbS films and due to the imbalance of the chemical deposition process, as well as the impact of the chemical nature of the substrates on their nucleation and growth. However, as noted by most researchers [17,38,64,65], it is critically necessary to obtain information about the magnitude of mechanical stresses at the „film−substrate“ interface (external stresses) caused by the difference of temperature coefficients of linear expansion and mismatch of the parameters of the crystal lattice of the film and substrate and the significant the difference of their thickness. These stresses belong to the second group.

Significant deformations are caused by exceeding the value of a certain critical level of mechanical stresses, inevitably leading to cracking or peeling of the film from the substrate, the occurrence of various kinds of defects, which significantly worsens the functional properties of the manufactured thin-film structures [66,67]. For this reason, the approximation (6) was used in this paper for calculating mechanical stresses due to mismatch of crystal parameters in the selected part of the thin film and the substrate, suggesting that the film dimensions allow considering the selected part as individual, although the existing texture mismatch requires additional studies. The temperature coefficient of linear expansion β of the substrates used [35], the thickness of the substrate (h_{substr}) and the film (h_{PbS}) are given in Table 3.

It can be seen from the table that the mechanical stresses $\sigma_{\Delta\alpha}$ occurring at the boundary between the film and the substrate have a negative value, i.e. the PbS films deposited on the discussed substrates experience mechanical compression stresses. The dependence of the mechanical stresses occurring at „film−substrate“ interface indicates that the stresses acting on the film on the fused quartz $\sigma_{\Delta\alpha}$ exceed the stresses on the sapphire by approximately 1.5 times and exceed the stresses on the photographic glass by 1.8 times. This is 5.9 times more than in a PbS film grown on the surface of a slide glass, although the temperature coefficient of linear expansion of a quartz substrate is ~ 15 times less. The results obtained are due to the fact that the calculated value of mechanical compression stresses, in addition to the temperature coefficient of linear expansion, is also determined by the ratio of the thickness of the film and the substrate.

As already noted, the division of stresses into internal and external is quite conditional, since the same factor can contribute to the development of stresses both during the nucleation and growth of films and at the „film–substrate" interface. Both types of stresses are caused by a number of influencing factors: differences in the temperature coefficients of linear expansion of the film and the substrate, inconsistencies in the parameters of their crystal lattices, as well as crystallographic defects present in the film.

Conclusion

Polycrystalline PbS films were obtained by chemical deposition on substrates of fused quartz, photographic glass, slide glass and synthetic sapphire, indicating the decisive impact of the substrate material on their morphology, composition, structure and optical properties, as well as the nature and magnitude of mechanical stresses occurring in them.

X-ray diffraction found that PbS films have a cubic structure $B1$ (space group $Fm\bar{3}m$) regardless of the substrate used. The formation of films deposited on substrates of fused quartz and sapphire occurs entirely from crystallites with a predominant orientation in the direction of (111) relative to the substrate, and up to 35.5 and 20.9% of crystallites with orientation (220), respectively, are present on the photographic glass and slide glass in addition to crystallites with orientation (111). The calculated average internal microstresses in the volume of PbS films are 3–9 times lower than stresses in chemically deposited films and nanocrystals of lead sulfide established by foreign researchers.

The results of AFM studies of the surface of quartz, photographic glass, slide glass and sapphire after etching in hydrofluoric acid and applying PbS films to them demonstrate, firstly, the scale dependence of the microrelief of both the substrate surface and films; secondly, the relief of the film coating does not inherit the relief of the substrate. PbS lead sulfide film with maximum roughness deposited on the surface of a quartz substrate can be recommended as a sensor element for monitoring toxic compounds in gaseous and aqueous media.

Optical studies showed that the band gap width of the film on fused quartz is close to the values for single crystal lead sulfide, which is associated with the existence of large ($\sim 1\,\mu$m) crystallites in the film. E_g increases as the grain size decreases. At the same time, the substrate material on which PbS was deposited has little effect on E_g.

It is shown that mechanical compression stresses occur at the „film–substrate" interface, which grow in a row slide glass ($-53.9\,\mathrm{kN/m^2}$)–photographic glass ($-181.4\,\mathrm{kN/m^2}$) – sapphire ($-212.4\,\mathrm{kN/m^2}$)–fused quartz ($-318.6\,\mathrm{kN/m^2}$), due to differences in the temperature coefficients of linear expansion of the film and substrate, as well as the ratio of their thickness. The results of studies of mechanical stresses can be used for the selection of substrate material for opto- and nanoelectronics, sensors and solar energy devices.

Funding

The study was funded by the Ministry of Science and Higher Education of the Russian Federation, the state contract № FEUZ-2023-0021 (H687/42B.325/23). Part of the work related to the study of crystal structure and optical properties was performed within the framework of the state assignment of the Ministry of Education and Science of the Russian Federation (topic „Spin", № 122021000036-3, and topic „Stream" № 122021000031-8).

Conflict of interest

The authors declare that they have no conflict of interest.

References

[1] J. Singh. *Electronic and optoelectronic properties of semiconductor structures* (Cambridge University Press, 2007)
[2] M.Y.H. Thabit, N.M.S. Kaawash, D.I. Halge, P.M. Khanzode, V.N. Narwade, J.W. Dadge, S.S. Dahiwale, K.A. Bogle. Mater. Today: Process., **92**, 876 (2023). DOI: 10.1016/j.matpr.2023.04.457
[3] E. Pentia, L. Pintilie, I. Matei, T. Botila, I. Pintilie. Infrared Phys. Technol., **44**, 207 (2003). DOI: 10.1016/S1350-4495(02)00225-6
[4] Q. Lv, R. Li, L. Fan, Z. Huang, Z. Huan, M. Yu, H. Li, G. Liu. Sensors, **23**, 8413 (2023). DOI: 10.3390/s23208413
[5] D.G. Moon, S. Rehan, D.H. Yeon, S.M. Lee, S.J. Park, S.J. Ahn. Sol. Energy Mater. Sol. Cells, **200**, 109963 (2009). DOI: 10.1016/j.solmat.2019.109963
[6] B. Jiang, X. Liu, Q. Wang, J. Cui, B. Jia, Y. Zhu, J. Feng, Y. Qiu, M. Gu, Z. Ge, J. He. Energy Environ. Sci., **13** (2), 579 (2020). DOI: 10.1039/C9EE03410B
[7] P.M. Khanzode, D.I. Halge, V.N. Narwade, J.W. Dadge, K.A. Bogle. Optik, **226**, 165933 (2021). DOI: 10.1016/j.ijleo.2020.165933
[8] V.F. Markov, L.N. Maskayeva. ZhAKh, **56** (8), 846 (2001) (in Russian).
[9] Z. Mamiyev, N.O. Balayeva. Mater. Today Sustain., **21**, 100305 (2003). DOI: 10.1016/j.mtsust.2022.100305
[10] N. Zhu, A. Zhang, Q. Wang, P. He, Y. Fang. Electr.: Int. J. Dev. Fundam. Practical Asp. Electr., **16**, 577 (2004). DOI: 10.1002/elan.200302835
[11] A.El. Madani, R. Essajai, A. Qachaou, A. Raidou, M. Fahoume, M. Lharch. Adv. Mater. Process. Technol., **8**, 3413 (2022). DOI: 10.1080/2374068X.2021.1970986
[12] V.F. Markov, L.N. Maskaeva, E.V. Mostovshchikova, V.I. Voronin, A.V. Pozdin, A.V. Beltseva, I.O. Selyanin, I.V. Baklanova. PCCP, **24**, 16085 (2022). DOI: 10.1039/D2CP01815B
[13] V.F. Markov, L.N. Maskaeva, P.N. Ivanov. *Gidrokhimicheskoe osazhdenie plenok sul'fidov metallov: modelirovanie, eksperiment* (UrO RAN, Ekaterinburg, 2006) (in Russian).
[14] U. Chalapathi, S.H. Park, W.J. Choi. Mater. Sci. Semicond. Process., **134**, 106022 (2021). DOI: 10.1016/j.mssp.2021.106022
[15] A.P. Gaiduk, P.I. Gaiduk, A.N. Larsen. Thin Solid Films., **516**, 3791 (2008). DOI: 10.1016/j.tsf.2007.06.122

[16] A. Sanchez-Martinez, O. Ceballos-Sanchez, D.E. Guzmán-Caballero, J.A. Avila-Avendano, C.E. Pérez-García, M.A. Quevedo-López, R. Ramírez. Ceram. Int., **47**, 18898 (2021). DOI: 10.1016/j.ceramint.2021.03.230
[17] L.N. Maskaeva, A.V. Pozdin, V.F. Markov, V.I. Voronin. Semicond., **54** (12), 1309 (2020). DOI: 10.1134/S1063782620120209
[18] B. Abdallah, R. Hussein, N. Al-Kafri, W. Zetoun. Iranian J. Sci. Technol. A, **43**, 1371 (2019). DOI: 10.1007/s40995-019-00698-1
[19] J. Sahadevan, S.E. Muthu, K. Kulathuraan, S. Arumugam, I. Kim, G.B.S. Pratha, P. Sivaprakash. Mater. Today Proc., **64**, 1849 (2022). DOI: 10.1016/j.matpr.2022.06.311
[20] D.M.M. Atwa, I.M. Azzouz, Y. Badr. Appl. Phys. B, **103**, 161 (2011). DOI: 10.1007/s00340-010-4311-4
[21] A.S. Obaid, M.A. Mahdi, Z. Hassan. Optoelectron. Adv. Mater. Rapid Commun., **6**, 422 (2012).
[22] Q. Lv, R. Li, L. Fan, Z. Huang, Z. Huan, M. Yu, H. Li, G. Liu. Sensors, **23**, 8413 (2023). DOI: 10.3390/s23208413
[23] N.I. Fainer, M.L. Kosinova, Yu.M. Rumyantsev, E.G. Salman, F.A. Kuznetsov. Thin Solid Films, **280**, 16 (1996). DOI: 10.1016/0040-6090(95)08188-7
[24] A.E. Gorodetsky, A.V. Markin, V.L. Bukhovets, V.I. Zolotarevsky, R.H. Zalavutdinov, N.A. Babinov, A.M. Dmitriev, A.G. Razdobarin, E.E. Mukhin. Tech. Phys., **66** (2), 288 (2021). DOI: 10.1134/S1063784221020122
[25] E.R. Dobrovinskaya, L.A. Lytvynov, V. Pishchik. *Sapphire: material, manufacturing, applications* (Springer, NY., 2009)
[26] Electronic source. Available at: http://zcq-quartz.ru/quartz-1.html
[27] R. Velichko. SVCh-elektronika, **1**, 66 (2016) (in Russian).
[28] V.G. Butkevich, V.D. Bochkov, E.R. Globus. Prikladnaya fizika, **6**, 66 (2001) (in Russian).
[29] M.S. Mikhailenko, A.E. Pestov, M.V. Zorina, A.K. Chernyshev, N.I. Chkhalo, I.E. Shevchuk. J. Surf. Invest., **17**, 1338 (2023). DOI: 10.1134/S102745102306037X
[30] G. Hodes. *Chemical Solution Deposition Of Semiconductor Films* (CRC Press, 2002)
[31] H.M. Rietveld. J. Appl. Crystallogr., **2**, 65 (1969). DOI: 10.1107/S0021889869006558
[32] B.H. Toby, R.B. Von Dreele. J. Appl. Crystallogr., **46**, 544 (2013). DOI: 10.1107/S002188981300353
[33] A.G. Khovansky. Matematicheskoe prosveshchenie, **17**, 93 (2013) (in Russian).
[34] C.K. De, N.K. Misra. Indian J. Phys., **A71**, 535 (1997).
[35] M.J. Weber. *Handbook Laser Science and Technology* (CRC Press LLC, 2003)
[36] C. Douketis, Z. Wang, T.L. Haslett, M. Moskovits. Phys. Rev. B, **51**, 11022 (1995). DOI: 10.1103/PhysRevB.51.11022
[37] W.W. Scanlon. J. Phys. Chem. Solids, **8**, 423 (1959). DOI: 10.1016/0022-3697(59)90379-8
[38] F.D. Kasimov, A.E. Lyutfalibekova. Tekhnologiya i konstruirovanie v elektronnoj apparature, **1**, 1 (2002) (in Russian).
[39] G.K. Williamson, W.H. Hall. Acta Metall., **1**, 22 (1953). DOI: 10.1016/0001-6160(53)90006-6.
[40] N. Choudhury, B.K. Sarma. Bull. Mater. Sci., **32**, 43 (2009). DOI: 10.1007/s12034-009-0007-y
[41] M. Mozafari, F. Moztarzadeh, D. Vashaee, L. Tayebi. Physica E, **44**, 1429 (2012). DOI: 10.1016/j.physe.2012.03.006
[42] P. Patnaik. *Handbook of inorganic chemicals* (McGraw-Hill, NY., 2003)
[43] L.A. Manuilov, G.I. Klyukovsky. *Fizicheskaya himiya i himiya kremniya* (Vysshaya shkola, M., 1962) (in Russian).
[44] Z.Ya. Khavin, V.A. Rabinovich. *Kratkiy himicheskij spravochnik* (Khimiya, LO, 1978) (in Russian).
[45] A. De Leon, M.C. Acosta-Enríquez, S.J. Castillo, A. Apolinar-Iribe. J. Sulfur Chem., **33**, 391 (2012). DOI: 10.1080/17415993.2012.689481
[46] T. Tohidi, K. Jamshidi-Ghaleh, A. Namdar, R. Abdi-Ghaleh. Mater. Sci. Semicond. Process., **25**, 197 (2014). DOI: 10.1016/j.mssp.2013.11.028
[47] E. Pentia, L. Pintilie, T. Botila, I. Pintilie, A. Chaparro, C. Maffiotte. Thin Solid Films, **434**, 162 (2003). DOI: 10.1016/S0040-6090(03)00449-8
[48] V.F. Markov, L.N. Maskaeva. Russ. Chem. Bull., **62**, 1523 (2014). DOI: 10.1007/s11172-014-0630-7
[49] A. De Leon, M.C. Acosta-Enríquez, S.J. Castillo, A. Apolinar-Iribe. J. Sulfur Chem., **33**, 391 (2012). DOI: 10.1080/17415993.2012.689481
[50] V.V. Podlipnov, V.A. Kolpakov, N.L. Kazansky. Komp'yuternaya optika, **40**, 830 (2016) (in Russian). DOI: 10.18287/2412-6179-2016-40-6-830-836
[51] A. Keller, S. Facsko, W. Möller. J. Phys. Condens. Matter., **21**, 495305 (2009). DOI: 10.1088/0953-8984/21/49/495305
[52] A.H. Ayupova, R.R. Garafutdinov, A.V. Chemeris, R.F. Talipov. Vestnik Bashkirskogo un-ta, **17**, 1677 (2012) (in Russian).
[53] B. Duan, J. Zhou, Y. Liu, M. Sun. J. Semicond., **35**, 116001 (2014). DOI: 10.1088/1674-4926/35/11/116001
[54] M.Y. Mustafa, I. Hilmy, E.Y.T. Adesta. ARPN J. Eng. Appl. Sci., **10**, 9736 (2015).
[55] M.S. Mikhailenko, A.E. Pestov, M.V. Zorina, A.K. Chernyshev, N.I. Chkhalo, I.E. Shevchuk. Poverhnost'. Rentgen., sinkhrotr. i neitron. issled. **12**, 25 (2023) (in Russian). DOI: 10.31857/S1028096023120154
[56] D.S. Pashkevich. Chem. Phys., **13**, 993 (2019). DOI: 10.1134/S1990793119060083
[57] V.A. Moshnikov, Y.M. Tairov, T.V. Khamova, O.A. Shilova. *Zol'-gel' tekhnologiya mikro- i nanokompozitov* (Lan, SPb, 2013) (in Russian).
[58] B.M. Smirnov *Fizika fraktal'nykh klasterov* (Nauka, M., 1991) (in Russian).
[59] J. Feder. *Fractals* (Plenum Press, NY., 1988)
[60] D.P. Vlasyuk, A.I. Mamykin, V.A. Moshnikov, E.N. Muratova. FKhS, **41** (5), 745 (2015) (in Russian).
[61] Y. Wang, A. Suna, W. Mahler, R. Kasowski. J. Chem. Phys., **87**, 7315 (1987). DOI: 10.1063/1.453325
[62] A.N. Weiss. Nauchno-Tekhicheskie Vedomosti SPbGPU, **213**, 9 (2015) (in Russian).
[63] L.B. Freund, S. Suresh. *Thin film materials: stress, defect formation and surface evolution* (Cambridge university press, 2004)
[64] L.N. Maskaeva, V.F. Markov, E.A. Fedorova, M.V. Kuznetsov. Russ. J. Appl. Chem., **91** (9), 1528 (2018). DOI: 10.1134/S1070427218090161
[65] A.R. Shugurov, A.V. Panin. Technical Phys., **65** (12), 1881 (2020). DOI: 10.1134/S1063784220120257
[66] G.E. Ayvazyan. Izv. NAN RA and GIUA. Ser. TN., **53** (1), 63 (2000) (in Russian).
[67] N.A. Dyuzhev, A.A. Dedkova, E.E. Gusev, A.V. Novak. Izv.vuz. Elektronika, **21** (4), 367 (2016) (in Russian).

Translated by A.Akhtyamov